

Original Article

KINETIC STUDIES ON CRYSTALLIZATION PROCESS OF AMORPHOUS VILAZODONE HYDROCHLORIDE

PRAVEEN CH*, ARTHANAREESWARI M, RAVIKIRAN A, KAMARAJ P, PAVAN KV

Department Of Chemistry, Srm University, Srm Nagar, Kattankulathur, Tamilnadu, Pin 603203, India.
Email: c.pvn002@gmail.com

Received: 14 Apr 2014 Revised and Accepted: 20 May 2014

ABSTRACT

Objective: In this study, crystallization kinetics of the amorphous Vilazodone hydrochloride (VLH) was investigated using Differential Scanning Calorimetry (DSC). Crystallization kinetics was assessed both under isothermal and non-isothermal mode and the data was evaluated to understand mechanism underlying in the devitrification.

Methods: For isothermal kinetics analysis Avrami method and for non-isothermal kinetics analysis Ozawa, Kissinger, Flynn-Wall-Ozawa and Augis-Bennett have been used. Moreover, the Powder X-Ray Diffraction (PXRD) and Scanning Electron Microscopy (SEM) were used to characterize the amorphous form and the resulted crystalline form.

Results: In isothermal kinetics process, the average calculated value of Avrami exponent (n) was found to be 2.6, indicating that the crystallization mechanism was diffusion control with a three-dimensional crystal growth. In case of non-isothermal process, the calculated value of Ozawa exponent (m) was found to be in the range of 2.4 to 3.5 and indicating that the crystallization is a result of nucleation and growth process. Further, the decreasing trend of Ozawa exponent (m) shows decrease in nucleation rate due to nucleation saturation. The calculated activation energy for isothermal kinetics analysis was found to be 18.4 kJ/mol. However, the average value of calculated activation energy values obtained from Kissinger, Flynn-Wall-Ozawa and Augis-Bennett methods in non-isothermal process was found to be 20.2 kJ/mol, which is close to that of the isothermal crystallization process.

Conclusion: The isothermal and non-isothermal crystallization kinetic parameters of A-VLH indicating, the crystallization mechanism is mainly diffusion controlled and three dimensional crystal growths during the amorphous to crystalline phase transformation. The average activation energy value of isothermal crystallization is close to that of the non- isothermal crystallization process.

Keywords: Vilazodone Hydrochloride; Crystallization kinetics; Amorphous; Differential Scanning Calorimetry; Avrami exponent.

INTRODUCTION

Majority of active pharmaceutical ingredients (APIs) can exist in different solid-state forms like crystalline (polymorphs, solvates) and amorphous state [1]. Amorphous solids do not have repetitive arrangement and thus have disordered internal arrangement; these disordered amorphous systems differ in solubility, stability, dissolution properties and compression characteristics from the more traditionally used crystalline counterparts and provide attractive alternatives to them in drug delivery formulation [2]. Amorphous form of APIs exhibits higher bioavailability than their crystalline counterparts. This advantage often suggests the formulator to the select amorphous form as a final drug substance for pharmaceutical dosage form development [3]. However, lower physical and chemical stability of amorphous form leaves a threat in view of product performance and efficacy [4]. Therefore, it is important to thoroughly assess the develop-ability of amorphous form as drug substance for the product.

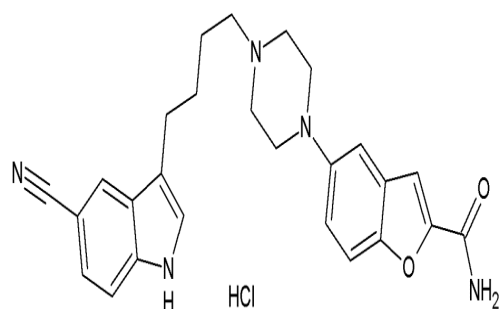


Fig. 1: Chemical structure of VLH

Vilazodone Hydrochloride (VLH) (Figure 1), 2-benzofurancarboxamide, 5-[4-[4-(5-cyano-1H-indol-3-yl) butyl]-1-piperazinyl]-, hydrochloride (1:1), is a selective serotonin reuptake inhibitor (SSRI) and a 5-HT_{1A} receptor partial agonist used for the treatment of major depressive disorder [5]. Amorphous form of Vilazodone Hydrochloride (A-VLH) is preferred for its dosage from development, anticipating better biopharmaceutical performance due to the higher dissolution rate of amorphous form over its crystalline form and also intellectual property is the concerns in pharmaceutical companies to select the alternative solid forms to enter into the various regulatory markets. In the present investigation, we studied the crystallization mechanism of VLH in an attempt to develop a pharmaceutical product of amorphous VLH. Pharmaceutical product development comprises of various unit operations that can subject the amorphous VLH to stress conditions of higher temperature and humidity. Hence it is very important to understand the crystallization mechanisms under both isothermal conditions and non-isothermal conditions, as isothermal conditions can be resulted during the shelf-life and non-isothermal conditions can be resulted during unit operations such as spray drying and melt granulation. These mechanism will help in designing the product development to ensure that amorphous VLH remains so till it is consumed by the consumer. Crystallization mechanism is established using Differential Scanning Calorimetry (DSC). Powder X-Ray Diffraction (PXRD) and Scanning Electron Microscopy (SEM) were also used to substantiate the findings.

THEORETICAL CONSIDERATION

Isothermal crystallization

The Isothermal crystallization kinetics of A-VLH has been studied using Johnson-Mehl-Avrami (JMA) theoretical model to determine the Avrami exponent ' n '. The crystallization fraction (X_t) can be described as a function of time (t) according to the formula [6-8].

$$X_t = 1 - \exp \left[-(Kt)^n \right] \quad (1)$$

$$\ln[-\ln(1 - X_t)] = \ln K + n \ln t \quad (2)$$

Where n is the Avrami component, which reflects both the crystallization mechanism and the dimensionality of the crystallization process; t is the annealing time; where K is the Avrami constant which is dependent on the nucleation rate and the growth rate, which is usually assigned by Arrhenian temperature dependence..

$$K = K_0 \exp \left(\frac{-E_c}{RT} \right) \quad (3)$$

$$\ln(K) = \ln K_0 - \frac{E_c}{RT} \quad (4)$$

Where E_c is the activation energy of crystallization, which describes the overall crystallization process, R is the universal gas constant and K_0 is frequency factor.

Non-isothermal crystallization

Based on the Avrami equation, several methods have been suggested to understand the nucleation and growth process using non-isothermal crystallization thermal data. Ozawa extended the Avrami equation to the non-isothermal condition [9-11]. Assuming that non-isothermal crystallization process may be composed of infinitesimally small isothermal crystallization steps, the following equation has been derived.

$$1 - X_t = \exp \left(\frac{-K^*}{\beta^m} \right) \quad (5)$$

$$\ln[-\ln(1 - X_t)] = -m \ln \beta + \ln K^* \quad (6)$$

Where, X_t is the relative crystallinity at temperature T , m is Ozawa exponent, which provides information about nucleation and growth process, K^* is a heating or cooling function related to overall crystallization rate and indicates how fast crystallization occur and β is heating or cooling rate.

In Ozawa's analysis, the exponent m is assumed to be constant and independent of temperature. From the plot of $\ln[-\ln(1 - X_t)]$ vs $\ln \beta$, the kinetic parameters m and K^* can be determined from the slope and intercept, respectively.

Kissinger and Augis-Bennett methods have been used to calculate activation energy of the Amorphous to crystalline phase transformation in non-isothermal crystallization process [12].

According to Kissinger model [13], the activation energy (E_a) of phase transformation can be determined using DSC experiment carried out with various heating rates and using the following equation:

$$\ln \left(\frac{\beta}{T_p^2} \right) = -\frac{E_a}{RT_p} + C \quad (7)$$

Where T_p is the crystallization peak temperature for a given heating rate β , E_a is the activation energy, R is the gas constant. From the plot of $\ln(\beta/T_p^2)$ vs $1000/T_p$, the activation energy E_a can be determined from the slope.

The activation energy E_a of phase transformation can also be obtained from Augis-Bennett method [14]. From the plot of $\ln(\beta/T_p)$ vs $1000/T_p$, the activation energy E_a can be determined from the slope.

$$\ln \left(\frac{\beta}{T_p} \right) = -\frac{E_a}{RT_p} + C \quad (8)$$

Flynn-Wall-Ozawa (FWO) is another effective method [15, 16] to calculate the activation energy using DSC non-isothermal curves. The equation can be expressed as

$$\ln(\beta) = -1.052 \frac{E_a}{RT_p} + C \quad (9)$$

A linear relationship is observed by plotting $\ln(\beta)$ vs $1000/T_p$ and the activation energy (E_a) can be obtained from the slope of the straight line.

MATERIALS AND METHODS

Material

The Amorphous form of Vilazodone Hydrochloride used in this study was supplied from Clearsynth (India) and the amorphous nature was confirmed by PXRD and DSC. The A-VLH is stored in refrigerator (2 to 8° C) in a closed container, to avoid any polymorphic transformations due to the temperature and humidity.

Methods

Differential Scanning Calorimetry

Isothermal and non-isothermal crystallization kinetics study was conducted using a Modulated Differential Scanning Calorimeter from model-TA Instruments (Q1000) (New Castle DE 19720, USA) equipped with refrigerated cooling accessory. The temperature and heat flow was calibrated using Indium. All measurements were performed by taking 2 to 3 mg of samples encapsulated into aluminum sample pans with pierced aluminum lid. The measurements were conducted under nitrogen with a purging rate of 50 mL/min.

Isothermal and non-isothermal crystallization processes

Isothermal crystallization study was performed by equilibrating the A-VLH samples from 30°C to specified temperatures, 150, 153, 155, 160 and 165 °C. Then measured the heat released with respective to time. Whereas non-isothermal crystallization kinetics was studied by heating the A-VLH from 30 °C to 300 °C at a constant heating rates of 5, 7.5, 10, 15 and 20 °C/min, respectively. The exothermic crystallization peaks were recorded as a function of temperature to analyze the non-isothermal crystallization kinetics.

Powder X-ray Diffraction (PXRD)

The experiments were carried out using PANalytical X'Pert PRO X-ray Powder Diffractometer (Eindhoven, Netherlands) using copper radiation $K\alpha_1$ with X'Celerator detector. The instrument was calibrated using NIST standard reference material 1976a (Corundum) for relative intensities and 640C (Silicon) for Peak position. Each diffraction profile was collected using following setting parameters of the diffractometer: the X-Ray tube was operated at a voltage of 40 kV and current of 30 mA; Ni filtered Cu $K\alpha_1$ radiation ($\lambda=1.5418 \text{ \AA}$); scan type - continuous mode; scan range (2θ) 2° to 50°; step size 0.03° 2θ ; time per step 50.0 sec. Data acquisition and analysis were performed on X'pert data collector and HighScore Plus software's, respectively.

Scanning electron microscopy (SEM)

SEM (JEOL Model JSM-6380) (Tokyo, Japan) analysis was done by dispersing the sample on carbon adhesive aluminum stubs and splutter coated with Platinum under vacuum by using JEOL auto fine coater (Model JFC-1600). The specimens were directly observed under microscope at an acceleration voltage of 2.0 kV using back-scattered electron detector and collected the images at same magnification for both amorphous and crystallized samples of VLH.

RESULTS AND DISCUSSION

Isothermal crystallization

Typical crystallization exotherms of A-VLH collected during isothermally at temperatures ranging from 150°C to 165°C are shown in Figure 2. The volume fraction crystallized (X_t) was calculated from these thermograms, using the following equation [17].

$$X_t = \frac{Q_t}{Q} \quad (8)$$

Where Q is the total area of the exothermic peak between the time t_i and t_f , where t_i and t_f are the start and end temperatures of crystallization. And, Q_t is the area between t_i and t .

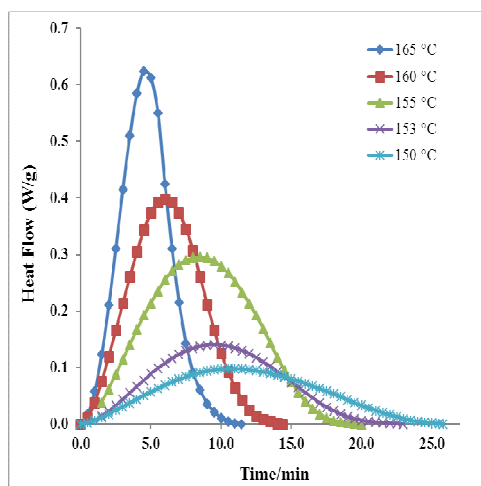


Fig. 2: DSC Isothermal curves of A-VLH at Various Crystallization temperatures

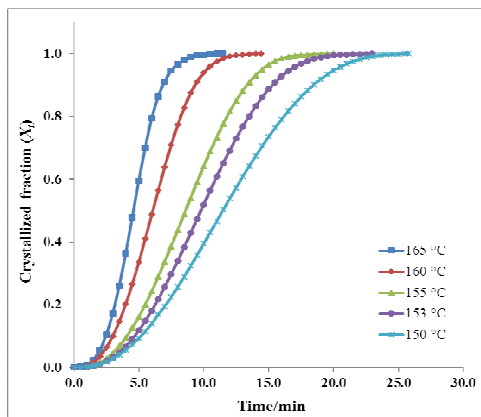


Fig. 3: The plot of crystallized fraction (X_t) of A-VLH as a function of time at different crystallization temperatures

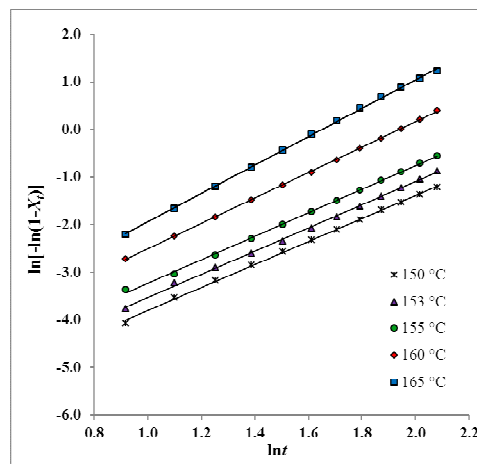


Fig. 4: Plots of $\ln[-\ln(1 - X_t)]$ vs $\ln(t)$ for the isothermal crystallization of A-VLH at the specified temperatures

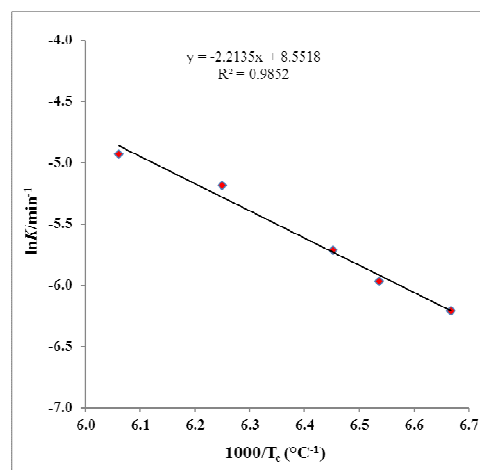


Fig. 5: Arrhenius plots of $\ln K$ vs $1/T_c$ for A-VLH

The evaluation of the volume fraction crystallized (X_t) against crystallization time during isothermal crystallization process showed (Figure 3) a typical sigmoidal curve shape.

The crystallization kinetics parameters during isothermal process were determined according to the equation 2 are showed in Figure 4. From the plot of $\ln[-\ln(1 - X_t)]$ vs $\ln(t)$ at various temperature, the Avrami exponent (n) and the crystallization rate constant K are obtained from the slope and intercept, respectively, the values are listed in table 1.

The activation energy of crystallization E_c was determined by the linear regression of the experimental data of $\ln K$ against $1/T_c$ from equation 4 and plotted in Figure 5. The value of crystallization activation energy is found to be 18.4 kJ/mol.

Table 1: Isothermal crystallization kinetic parameters and activation energy (ΔE) of A-VLH

Sample	T_c (°C)	$t_{0.5}$ (min)	K (min ⁻¹)	n	ΔE (kJ/mol)
A-VLH	150	11.3	2.0×10^{-3}	2.4	-18.4
	153	9.9	2.6×10^{-3}	2.4	
	155	8.6	3.3×10^{-3}	2.5	
	160	6.1	5.6×10^{-3}	2.7	
	165	4.6	7.2×10^{-3}	3.0	

The crystallization half-time ($t_{0.5}$) is another important kinetic parameter, defined as the time at which relative crystallinity X_t is 50%. The half-time of crystallization [18] ($t_{0.5}$) can be calculated according to the following equation.

$$t_{0.5} = \left(\frac{\ln 2}{K} \right)^{1/n} \quad (9)$$

The values of $t_{0.5}$ are reported in table 1. The value of Avrami exponent n (table 1) can reflect both the crystallization mechanism and the dimensionality of the crystallization process. The n values were found in the range of 2.4-3.0 which can represent a 'diffusion

controlled three-dimensional growth' during the crystallization [19]. The K values are dependent on the nucleation rate and the growth rate and extremely sensitive to T_c . The value of K increases with increase in T_c and the longer the crystallization half-time ($t_{0.5}$) the lower the rate of the crystallization.

Non-Isothermal crystallization

The typical non-isothermal DSC thermograms of A-VLH obtained by heating the sample at rate of 5, 7.5, 10, 15 and 20 °C/min, the plots are represented in Figure 6. The data suggesting that increase in heating rate (β) resulted wider exothermic trace and shift towards higher temperatures. The characteristic observations are plotted in table 2.

Table 2: Crystallization peak maximum values at different heating rates and Non-Isothermal crystallization kinetic parameters based on Ozawa analysis of A-VLH

β (°C/min)	T_p (°C)	Parameter	Temperature (°C)			
			178	180	182	184
5	173.23	m	3.5	3	2.7	2.4
7.5	177.66	$\ln K^*$	6.5	5.9	5.8	5.4
10	181.73					
15	186.85					
20	190.20					

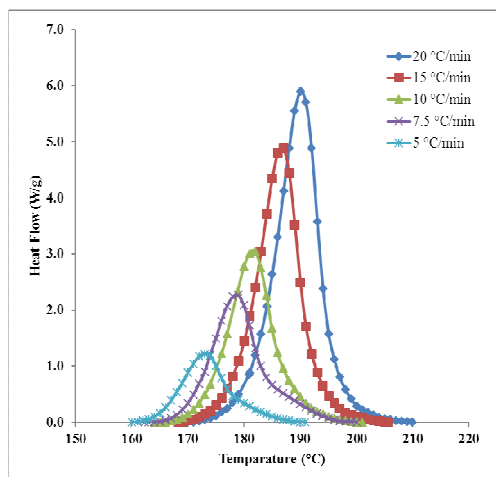


Fig. 6: DSC Non-isothermal crystallization exotherms of A-VLH at different heating rates

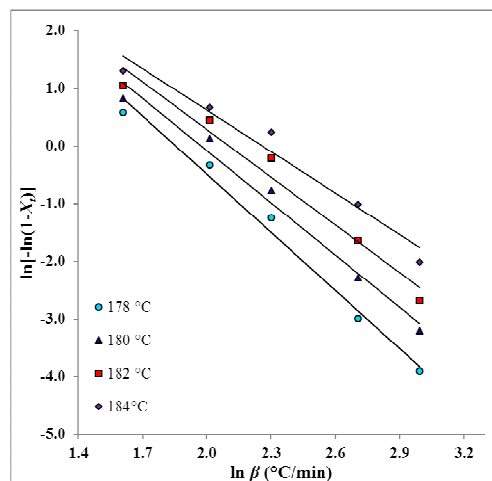


Fig. 8: Plots of $\ln[-\ln(1 - X_t)]$ vs $\ln \beta$ for the non-isothermal crystallization of A-VLH at the specified temperatures

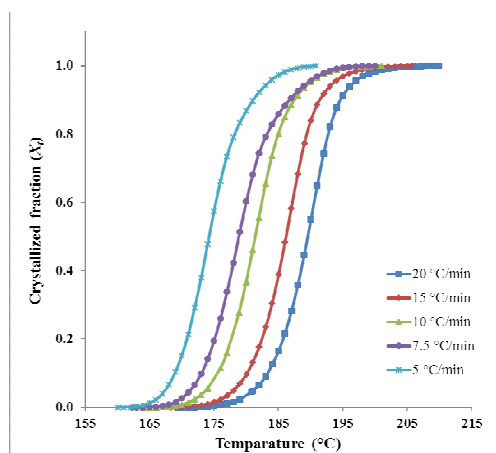
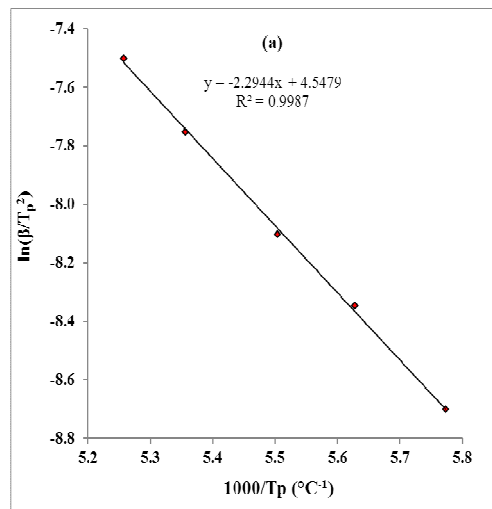


Fig. 7: The plot of crystallized fraction (X_t) of A-VLH as a function of Temperature at different heating rates



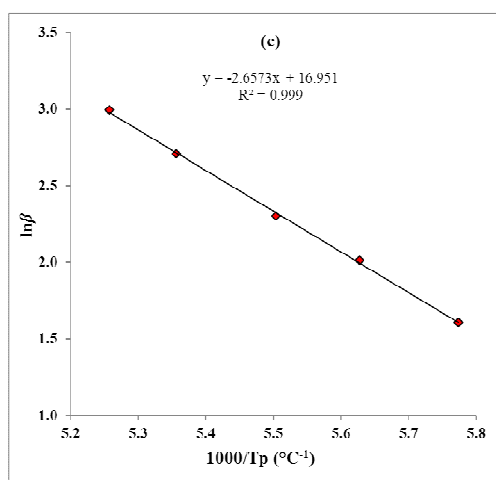
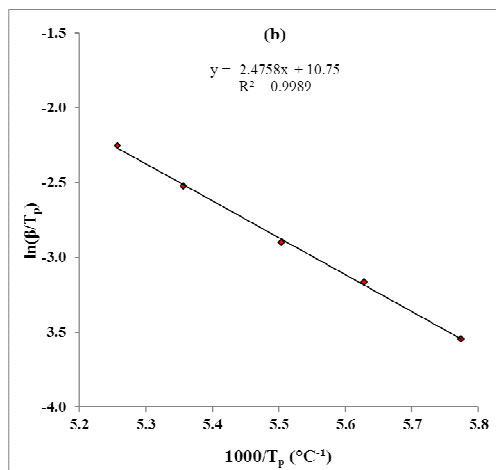


Fig. 9: (a) Kissinger (b) Augis-Bennett (AB) (c) Flynn-wall-Ozawa (FWO) plots for evaluating the activation energy for non-isothermal crystallization of A-VLH

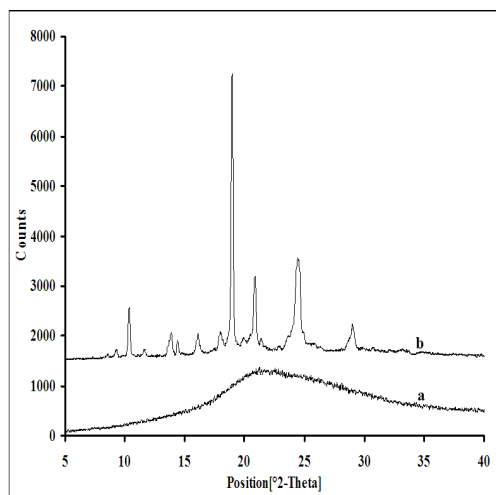


Fig. 10: Powder X-ray diffraction patterns for the (a) Amorphous form and (b) crystallized powdered samples of VLH

The crystallized fraction, X_t , was calculated from the exothermic peaks of non-isothermal crystallization process using equation 8. The crystallized fraction plotted as a function of temperature was showed in Figure 7. It is observed that all the curves have the same sigmoidal shape. By plotting $\ln[-\ln(1-X_t)]$ vs $\ln\beta$ at a set of specific

temperatures according to equation 6, a series of straight lines were obtained (Figure 8), the kinetic parameters m and K^* were determined from the slope and intercept, respectively, and compiled in table 2. It is clear from table 2 that the Ozawa exponent (m) decreases with increase in temperature, which indicates that crystallization process of A-VLH is associated with nucleation and growth process. The decrease trend of Ozawa exponent (m) shows the decrease in the nucleation rate due to nucleation saturation. The activation energy (E_a) values were calculated using Kissinger's, Augis-Bennett(AB) and Flynn-wall-Ozawa (FWO) methods, and plotted as $\ln(\beta/T_p^2)$ vs $1000/T_p$, $\ln(\beta/T_p)$ vs $1000/T_p$ and $\ln(\beta)$ vs $1000/T_p$ (represented in Figure 9) using equation 7, 8 and 9 respectively, the results are compiled in table 3. The average calculated value of activation, using these methods, was found to be 20.2 kJ/mol.

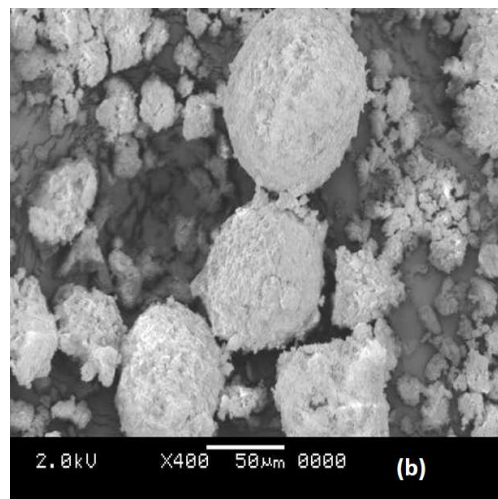
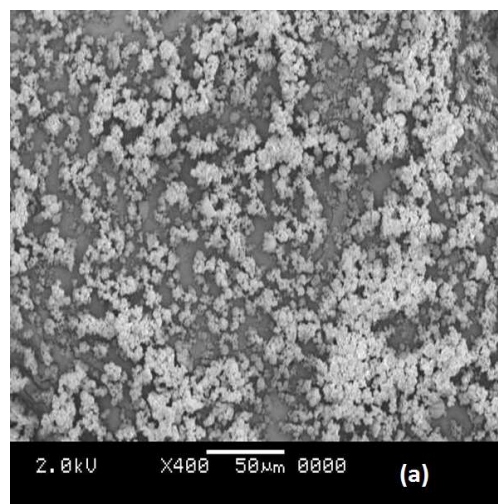


Fig. 11: SEM images for the (a) Amorphous form and (b) crystallized powdered samples of VLH

Characterization by PXRD and SEM

A-VLH and the crystallized solid (C-VLH), obtained after thermal treatment were characterized using PXRD and SEM techniques. An overlaid PXRD pattern of A-VLH and C-VLH was shown in Figure 10. A typical broad hallow type PXRD profile with no sharp peaks was observed in case of A-VLH and that confirming the amorphous nature. The PXRD profile of the C-VLH was matching with that of polymorphic form-VII of VLH, which was

previously reported in literature [20]. The C-VLH PXRD profile has major characteristic peaks appeared at 10.36°, 13.86°, 16.11°, 18.0°, 18.98°, 20.86°, 24.09°, 24.59°, 24.80° and 29.02° $2\theta \pm 0.2^\circ$. A comparative evaluation of morphologies in SEM images (Figure 11) of both A-VLH and C-VLH indicated that the

C-VLH, which was resulted after thermal analysis by DSC, was having bigger particle size, with nearly spherical shaped solid matter. The SEM observations support the kinetics analysis results related to mechanism, that the crystallization growth was three dimensional.

Table 3: The activation energy for crystallization (E_a) obtained by different non-isothermal methods

Non-Isothermal model	Activation energy of crystallization (kJ/mol)
Kissinger	-19.1
Augis-Bennett	-20.6
Flynn-wall-Ozawa	-21.0
Average value	-20.2

The disordered molecular arrangement in amorphous form contributes excess properties (i.e. enthalpy, entropy, and free energy) [4] which act as a constant driving force for loss of energy and regain of order by reverting to the thermodynamically stable crystalline form. The dissipation of this energy could be enhanced to a variable extent in the presence of different stress-inducers during manufacturing process of solid dosage form. The presently investigated crystallization behavior of A-VLH in the presence of isothermal and non-isothermal condition would allow for adoption of suitable high viscous polymers that either prevent or retard Active pharmaceutical ingredient (API) recrystallization by increasing the activation energy. The incorporation of certain polymers with amorphous API to make the amorphous sold dispersion (ASD) is generally found to increase the physical stability of the amorphous API and provide improvements in dissolution rates. Thus, from a physical stability standpoint it is preferable to use the ASD rather than the amorphous API.

REFERENCES

- Vippagunta SR, Brittain HG, Grant DJ. Crystalline solids. Adv Drug. Deliv Rev. 2001; 48(1): 3-26.
- Kaushal AM, Gupta P, Bansal AK. Amorphous drug delivery systems: molecular aspects, design, and performance. Crit Rev Ther Drug Carrier Syst. 2004; 21(3):10.
- Dwived SD, inventor; Cadila healthcare limited, assignee. Amorphous form of Vilazodone hydrochloride and process for its preparation. WIPO Patent No. 2012131706. 2012 Oct 04.
- Yu L. Amorphous pharmaceutical solids: preparation, characterization and stabilization. Adv Drug Delivery Rev. 2001; 48(1):27-42.
- Cruz MP. Vilazodone HCl (Viibryd): A Serotonin Partial Agonist and Reuptake Inhibitor for the Treatment of Major Depressive Disorder. Pharmacy and Therapeutics. 2012; 37(1): 28-31.
- Avrami M. Kinetics of phase change. I General theory. J Chem Phys. 1939; 7(12): 1103.
- Avrami M. Kinetics of phase change. II. Transformation time relations for random distribution of nuclei. J Chem Phys. 1940; 8(2):212.
- Avrami M. Granulation, phase change, and microstructure kinetics of phase change. III. J Chem Phys. 1941; 9(2):177.
- Ozawa T. Kinetics of non-isothermal crystallization. Polym. 1971; 12(3): 150-158.
- Ozawa T. Nonisothermal kinetics of crystal growth from preexisting nuclei. Bull Chem Soc Jpn, 1984; 57(3):639-643.
- Ozawa T. Non-isothermal kinetics and generalized time. Thermochim Acta. 1986; 100(1):109-118.
- Qiao JC, Pelletier JM. Isochronal and isothermal crystallization in $Zr_{55}Cu_{30}Ni_5Al_{10}$ bulk metallic glass. Trans Nonferrous Met Soc China. 2012; 22(3):577-584.
- Kissinger HE. Reaction kinetics in differential thermal analysis. Anal chem. 1957; 29(11):1702-1706.
- Augis JA, Bennett JE. Calculation of the Avrami parameters for heterogeneous solid state reactions using a modification of the Kissinger method. J Therm Anal Calorim. 1978; 13(2):283-292.
- Flynn JH, Wall LA. A quick, direct method for the determination of activation energy from thermogravimetric data. J Polym Sci Part B: Polym Lett. 1966; 4(5): 323-328.
- Ozawa T. A new method of analyzing thermogravimetric data. Bull Chem Soc Jpn. 1965; 38:1881-1886.
- Jiang XL, Luo SJ, Sun K, Chen XD. Effect of nucleating agents on crystallization kinetics of PET. Express Polym Lett. 2007; 1(4):245-251.
- Li J, Zhou C, Wang G, Tao Y, Liu Q, Li Y. Isothermal and nonisothermal crystallization kinetics of elastomeric polypropylene. Polym test. 2002; 21(5): 583-589.
- Yang YJ, Xing DW, Shen J, Sun JF, Wei SD, He HJ, McCartney DG. Crystallization kinetics of a bulk amorphous Cu-Ti-Zr-Ni alloy investigated by differential scanning calorimetry. J alloy compd. 2006; 415(1): 106-110.
- Bathe A, inventor; Merck patent GMBH, assignee. Polymorphic forms of 1-4-(5-cyanoindol-3-yl) butyl-4-(2-carbamoyl benzofuran-5-yl) piperazine hydrochloride. WIPO patent no. 2002102794. 2002 Dec 27.